



HAL
open science

Further insight on amine-metal reaction in epoxy systems

Christophe Drouet, Fabrice Salles, Zineb Fritah, Olivier Marsan, Carole Thouron, Maëleonn Aufray

► **To cite this version:**

Christophe Drouet, Fabrice Salles, Zineb Fritah, Olivier Marsan, Carole Thouron, et al.. Further insight on amine-metal reaction in epoxy systems. *Surfaces and Interfaces*, 2021, 23, pp.100959. 10.1016/j.surfin.2021.100959 . hal-03138377

HAL Id: hal-03138377

<https://hal.science/hal-03138377>

Submitted on 11 Feb 2021

HAL is a multi-disciplinary open access archive for the deposit and dissemination of scientific research documents, whether they are published or not. The documents may come from teaching and research institutions in France or abroad, or from public or private research centers.

L'archive ouverte pluridisciplinaire **HAL**, est destinée au dépôt et à la diffusion de documents scientifiques de niveau recherche, publiés ou non, émanant des établissements d'enseignement et de recherche français ou étrangers, des laboratoires publics ou privés.

Further insight on amine-metal reaction in epoxy systems

Christophe Drouet^{1,*}, Fabrice Salles², Zineb Fritah¹, Olivier Marsan¹, Carole Thouron¹,
Maëlen Aufray^{1,*}

¹CIRIMAT, Université de Toulouse, INP, CNRS, UPS, Ensiacet, Toulouse, France

²ICGM, Univ. Montpellier, CNRS, ENSCM, Montpellier, France

*Main corresponding author:

Prof. Christophe DROUET (ORCID: 0000-0002-8471-8719)

CIRIMAT Institute

Université de Toulouse

Ensiacet, 4 allée Emile Monso

FR-31030, Toulouse, France

E-mail : christophe.drouet@cirimat.fr

Co-corresponding author :

Dr. Maëlen AUFRAY (ORCID: 0000-0001-5921-6322)

CIRIMAT Institute

Université de Toulouse

Ensiacet, 4 allée Emile Monso

FR-31030, Toulouse, France

E-mail : maelenn.aufray@ensiacet.fr

Abstract

Among thermosetting polymers, epoxy resins are major components of adhesives, sealants, paints and composites. Polymerization is often achieved by reaction of epoxy monomers like DGEBA with amine hardeners such as DETA. Previous works showed that polyamines interact with metal (hydr/oxide) substrates leading to the formation of an interphase involving the chelation of surface metal ions. In this work, we further explored the interaction between DETA and aluminum (hydr)oxide, denoted Al, via a combined experimental and modeling approach. We inspected in depth by DSC the modifications of glass transition temperature T_g and change in heat capacity ΔC_p after curing, allowing us quantifying the impact of Al amount on DGEBA/DETA degree of cure α . A new parameter, the “percentage of inhibition of cure” denoted $\bar{\alpha}$, was defined reaching up to ~4 % in our experimental conditions. In parallel, *in situ* mixing calorimetry confirmed the exothermic character of DETA interaction with Al with various degrees of division. DFT calculations were carried out to examine DETA/Al³⁺ chelates. Among plausible chelate configurations, one was associated with a lower conformational energy and shorted Al-N bond lengths, suggesting greater stability. Calculated and experimental Raman spectra were additionally investigated, allowing us to discuss further about the DETA/Al³⁺ chelates at play.

Keywords

Thermosetting resins, Interphase, Calorimetry, Modeling and simulation, Adhesion

1. Introduction

Epoxy resins occupy a decisive position in a large variety of industrial domains, from construction to transportation and sports, among others. They are key components of sealants and adhesives (e.g. Araldite® glues), paints/coatings and many light-weight composite matrices [1-3]. The polyepoxy resin is usually polymerized by reacting with polyamine curing agents to form the final epoxy networks.

In the presence of metal substrates, however, the amine precursor was found to react with metal surfaces [4-15], leading to significant modifications in terms of degree of curing and glass transition temperature, T_g . These modifications can in turn alter the expected behavior of the polymerized networks as well as their mechanical/thermal resistance over time and other properties upon use [6-8]. Such amine/metal interaction is both physical and chemical in nature, with the formation of an interphase domain between the metal surface and the liquid amine monomer. The occurrence of such interphases, implying monomers local accumulation and adsorption was essentially explored to-date indirectly (i.e. *postmortem*) by way of XPS and FTIR spectroscopies [12,13,15,16]. These techniques allowed observing the formation of metal-amine surface complexes [17-20] as well as of chelates in solution [6-8,17-19]. This was associated with partial dissolution of the metal surface on contact with the amine [17-21], leading to the presence of the metal element in the adhesive layer [10,14]. A molecular dynamics (MD) study has been reported to investigate an epoxy-amine-copper system and its curing kinetics [22]; also, another MD study investigated the DGEBA/DETA polymerization at the vicinity of a generic surface [23]. These works pointed to the need to further explore such systems by microscopic simulation approaches, so as to better understand relative molecular interactions. An acid-base mechanism of amine-aluminum interaction was tentatively proposed from experimental data [17-19], which was lately extended to a more general case [24], involving the formation of surface complexes and chelate release. But these steps still need to be explored in depth. Recently, amine/metal (hydr/oxide) interphase formation was examined for the first time by direct observations via *in situ* mixing calorimetry [24], using DETA as a model polyamine curing agent. Interphase formation was found to be associated with a net enthalpy of interaction clearly exothermic (contrarily to the epoxy/metal (hydr/oxide) system rather unreactive), and the nature of the metal (Al, Cu) and its oxidation state were directly linked to the intensity of the exothermic event.

Several types of chelates are susceptible to form, and their relative stability for a given polyamine may vary with the nature of the metal-based surface. In the present work, we have focused on the DETA/aluminum (hydr/oxide) system – two components often encountered

industrially in epoxy-based applications – and have combined differential scanning calorimetry (DSC), *in situ mixing* calorimetry, Raman microscopy and DFT calculations to further investigate the chelation and interphase formation processes at play.

2. Materials and methods

2.1. Materials

A batch of aluminum chips was obtained by drilling in an aluminum plate (2024 alloy, Rocholl GmbH), obtaining millimetric pieces. Aluminum powder 200 mesh was purchased from Acros (99% purity). The BET surface area of these two types of samples was respectively measured in this work at 0.7 and 3.7 m²/g (Marion technologies, France, using a pre-treatment of 250 °C for 2 h). Prior to use it was treated by contact with the atmosphere at 80°C for 14 h to obtain a stabilized “native oxide” layer. **Figure S1** (Supporting Information) reports the typical XRD pattern of the aluminum-based powder substrate used in this study. Data were acquired for 2 h using an Equinox 100 diffractometer (INEL) with a cobalt anticathode ($\lambda = 1.78897 \text{ \AA}$). The data match well with metallic Al (JCPDS file No.99-101-2989) with traces of derivatives such as Al(OH)₃ and AlO(OH) that correspond to (hydr)oxidized Al-based chemical species on the particles surface. For the sake of brevity, in the text, the terms “aluminum (Al)” or “metal” will be used to describe the substrates used without mentioning the surface (hydr)oxidation state – as is customary in this field.

Diethylenetriamine, DETA, was the polyamine used in this work as typical curing agent (Sigma-Aldrich, Molecular Weight: 103.17 g/mol, viscosity at 20°C: 7.16 mPa.s, functionality: 5 protons from 2 terminal primary amines and 1 intermediate secondary amine). DGEBA (Bisphenol A diglycidyl ether, DER 332, from Sigma-Aldrich, Molecular Weight: 340.41 g/mol, functionality: 2 epoxy groups) was used as the epoxy prepolymer. **Figure S2** reports the chemical composition of the DGEBA and DETA monomers used in this study.

2.2. Differential scanning calorimetry (DSC)

Differential scanning calorimetry (DSC) was used for the follow-up of glass transition temperatures (T_g) and the corresponding variations of heat capacity (ΔC_p). The experiments were run in dynamic conditions under nitrogen gas flow, using a DSC 204 Phoenix Series (NETZSCH, Selb, Germany) apparatus coupled with a TASC 414/4 controller. Calibration

was performed in terms of melting temperatures of In, Hg, Sn, Bi, CsCl, and Zn, via 2 subsequent +10 °C/min temperature ramps for reproducibility check. Cured samples to analyze were weighed with the accuracy of ± 0.1 mg in aluminum capsules. Aluminum pans containing 15–20 mg of polymer were heated two times from –50 °C to 200 °C at a heating rate of 10 °C/min under a continuous flow of nitrogen. The glass transition temperature was determined during the second run. The Proteus® Software allowed us to determine the “onset” and “endset” temperatures associated with the glass transition as well as the variation in heat capacity, ΔC_p , accompanying this event.

For these glass transition measurements, DGEBA/DETA networks were prepared by mixing the monomers in theoretical stoichiometric proportions, leading to bulk samples after 3 h of curing at room temperature and 1 h at 150°C. The molar stoichiometry ratio a/e between the amine and the epoxy was calculated based on the following equation:

$$r = \frac{a}{e} = \frac{f_a \cdot n_a}{f_e \cdot n_e} \quad \text{Eq. 1}$$

where a is the number of moles of amine chemical functions, e the number of moles of epoxide chemical function, n is the number of moles of amine or epoxy monomers and f is their corresponding functionality. Strict theoretical stoichiometry for the pure DETA/DGEBA system is thus obtained for $r = 1$. For studying the evolution of T_g and ΔC_p versus the mass of aluminum m_{Al} contacted with the DETA prior to polymerization with DGEBA, the DETA was retrieved (limpid supernatant) after the mixing calorimetry experiments. Experiments were run in triplicates.

A polyepoxy thin film was also prepared, by mixing DGEBA and DETA as before in stoichiometric amounts and applying the fresh mixture onto an aluminum plate. The thickness of the film was set to *ca.* 100 μm by positioning a 100 μm-thick wedge on both sides of the plate and rolling a glass stick onto the wedges for obtaining a thin layer of monomers mixture. The film was retrieved after 1 h of curing at 150°C followed by a waiting time of 24 h at room temperature.

2.3. Mixing calorimetry

Amine-metal interaction was followed *in situ* by mixing calorimetry at 40 °C thanks to a Setaram C80 calorimeter equipped with Calvet 3D sensors and using two-compartment

Hastelloy® mixing cells, as described elsewhere [24]. Briefly, the heat flow associated with the studied reaction occurring in the sample calorimeter cell was recorded over time taking the second empty calorimeter cell as reference. Each mixing cell consisted in two compartments separated by a Teflon® membrane. Upon lowering a helix-shaped piercing tool manually, membrane rupture allowed initiation of the reaction in the measuring cell. In this study, 1.5 ml of pure liquid DETA was placed in the upper compartment of the measuring cell and the desired amount (10 to 1000 mg) of aluminum powder specimen was placed in the lower compartment. Determination of the raw enthalpy of interaction was made by integration of the heat flow-versus-time signal after baseline stabilization. Typical experiment duration was of the order of one hour. The eventual asymmetry of the calorimeter setup was accounted for by way of a “blank” experiment run systematically after return of the baseline to its stabilized value, and the obtained ΔH_{blank} enthalpy value was subtracted from the raw measured enthalpy to determine the corrected reaction enthalpy (ΔH_{R}). Calorimeter calibration of the heat flow signal was checked regularly following the dissolution of dry potassium chloride (KCl, Merck) in water in the same experimental conditions (heat flow resolution: 0.10 μW , temperature accuracy: $\pm 0.1^\circ\text{C}$).

2.4. Raman microscopy

Raman microspectroscopy – Horiba Jobin Yvon LabRAM HR 800 – using a continuous argon laser emitting at 532nm (13 mW) was used to provide chemical and structural complementary characterization of the samples. The analyses were performed with a x100 magnification with a numerical aperture of 0.9, conferring a spot diameter of 0.8 μm and an axial resolution of 2.6 μm . No surface degradation or debris were detected under these conditions. The analyses were performed with a holographic network of 600 lines per mm, giving a spectral resolution of 2 cm^{-1} . Each spectrum was recorded on the 100-5000 cm^{-1} spectral range with 90 s acquisition time and 3 accumulations. All spectra were processed using the LabSpec6 software, including the baseline correction.

2.5. Computational modeling

Computational methods were used to probe, in a simplified model, the most stable configuration between aluminum and DETA. In these preliminary calculations, two hypotheses were made on the DETA and aluminum speciation as their exact states have not yet been established: DETA was considered in its -2 anionic divalent form (loss of two protons) and aluminum was considered interacting in its usual trivalent form Al^{3+} , leading to

Al/DETA complexes with a +1 overall charge. A geometry optimization procedure was performed for two relevant conformations of the DETA ion, as described in the text, by using density functional theory (DFT) simulations implemented in DMol³ [25].

Calculations were performed by considering the PBE GGA density functional [26], the double numerical basis set containing polarization functions on H atoms (DNP), and all electrons for the core treatment. The formal spin was used as initial for each atom since the calculations were performed with the spin unrestricted.

The convergence of the calculations was reached when variations were lower than 10⁻⁵ Ha for energy, 0.002 Ha/Å for maximal force, 0.005 Å for maximal displacement. From these optimized structures, it was possible to extract the most stable conformation from the conformational energy *E* of DETA in the corresponding Al/DETA chelates. Furthermore, Raman spectra were calculated with DMol³ using the same parameters. For the sake of comparison, the case of pure DETA was also calculated as a reference.

3. Results and discussion

3.1. Impact of amine-Al reaction on glass transition

Epoxy polymeric networks are obtained by reacting an epoxy resin exposing several epoxide functional groups with a curing agent, for example a polyamine. In this work, we selected two such precursors among the most widely encountered in industrial applications, namely the DGEBA epoxy resin (bisphenol A diglycidyl ether) and the DETA amine (diethylenetriamine). The reaction in stoichiometric relative amounts of these two monomers leads, after final polymerization, to 3D networks characterized by a glass transition temperature, *T_g*, of the order of 131 ± 2 °C (onset temperature, **Table 1 exp. #1**), as determined from DSC (see **Figure S3** for a typical example of DSC curves obtained). In contrast, this glass transition (onset) temperature is significantly lowered when the amine has been contacted with metal surfaces, as illustrated here the case of aluminum specimens with different degrees of division, i.e. in the form of plate, chips and powder (**Table 1 exp. #2–5**), as expected [4,5,6,8]. The *T_g* endset also globally followed this trend. It may be noted that, on the contrary, previous observation showed that pre-contacting DGEBA with Al did not lead to significant *T_g* modification [24]. This effect is thus related here to the amine-metal interaction.

Table 1. Glass transition temperature data (onset and endset) from DSC for the DGEBA/DETA/Al system in different conditions.

Exp. #	Experimental conditions	T _g onset (°C)	T _g endset (°C)
#1	DETA (1.5 ml)	131 ± 2	152 ± 4
#2	Al chips (586 mg) + DETA (1.5 ml)	110 ± 1	130 ± 1
#3	Al chips* (586 mg) + DETA (1.5 ml)	113 ± 1	136 ± 1
#4	Al powder (586 mg) + DETA (1.5 ml)	113 ± 2	141 ± 1
#5	Al plate** + DETA (1.5 ml)	96 ± 7	164 ± 18

* The Al chips were retrieved from exp. #2, washed in ethanol and oven-dried at 50 °C overnight

** A thin polyepoxy film (thickness ~ 100 µm) was prepared from DETA/DGEBA freshly mixed, as described in the experimental section

The evolution of T_g onset and endset were then followed versus the mass of Al powder, m_{Al}, contacted with the DETA monomer (1.5 mL or 1.4 g) prior to polymerization with DGEBA. **Figure 1a** reports the corresponding data per unit of contact surface. As a general trend, both the onset and endset glass transition temperature values followed a decreasing trend with the amount of Al. These results can be explained on the basis of a progressive departure from stoichiometry between the amine and epoxy functions described in **Eq. 1** ($a/e < 1$, [8]). Upon interaction with Al-based surfaces, some functionalities of the amine get involved in the chelation of aluminum and are thus not available anymore for polymerization with epoxide groups. From a molecular perspective, the decrease in crosslinking density increases the chain mobility thus decreasing the T_g [27]. From an industrial/applicative viewpoint, such a T_g decrease when the amine is contacted with metal-based surfaces may lead to apparently unexplained behaviors of the cured polyepoxy networks, and should be considered/anticipated in the formulation of paints and sealants, for example.

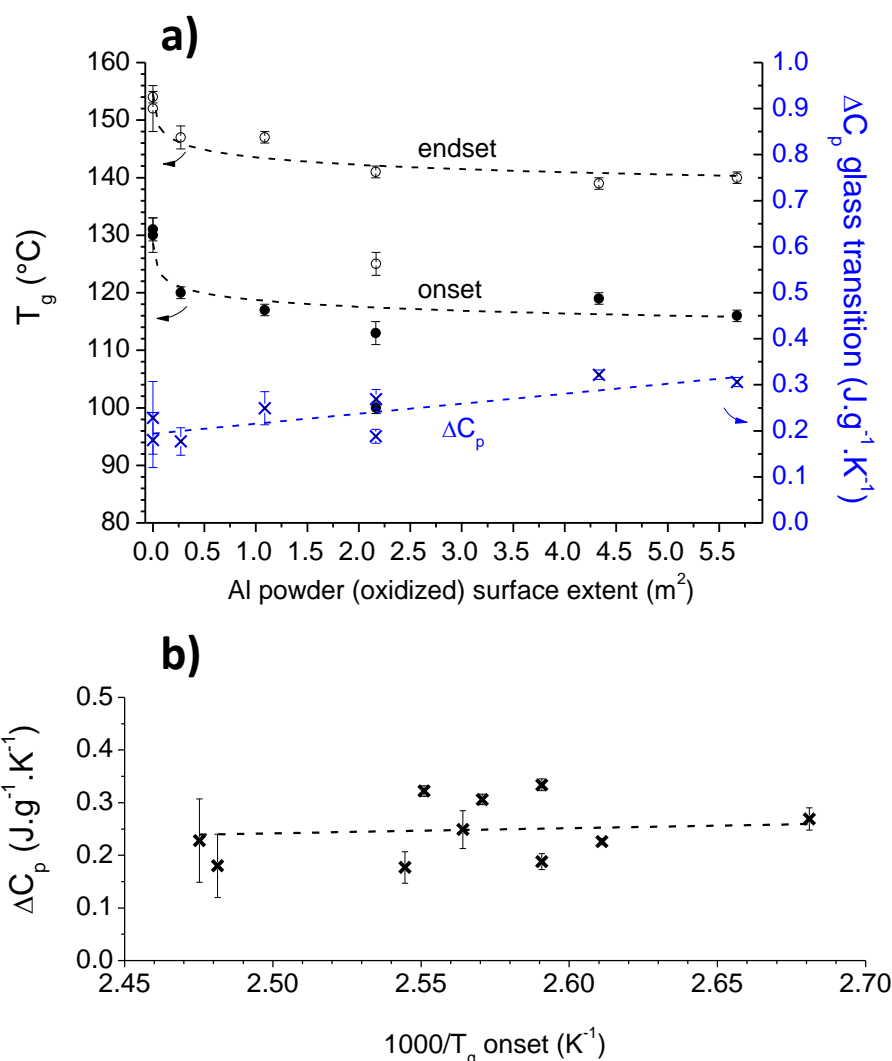


Figure 1. a) Evolution of T_g onset, endset and ΔC_p versus the surface extent of Al powder contacted with 1.5 mL DETA before polymerization with DGEBA (corresponding to 1.4 g DETA + 11.8 g DGEBA giving a polymer mass of 13.2 g) and b) Evolution of ΔC_p as a function of T_g onset ($R^2 = 0.6589$).

Besides T_g modification with the amount of Al, the change in heat capacity ΔC_p accompanying the glass transition was also followed (**Figure 1a**). Despite some data point scatter, presumably linked to the inhomogeneous distribution of the DETA/aluminum complexes within the liquid amine samples (retrieved after mixing calorimetry experiments – see next section – and analyzed by DSC), an increasing tendency may be suggested. A rather linear variation may indeed be unveiled for ΔC_p from *ca.* 0.18 up to $\sim 0.32 J.g^{-1}.K^{-1}$ over the mass range 0–1.2 g Al, although the correlation factor only reaches $R^2 = 0.6589$. This increase

can be seen as a consequence of molecular-scale modifications of the polymer 3D network after curing in the presence of chelated aluminum. A decrease of ΔC_p was already reported for polymers, including epoxys, when the degree of curing increases – thus for greater crosslinking densities. Indeed, upon curing, polymer chain stiffness increases leading to lower configurational entropy and therefore to ΔC_p decrease [27]. Our findings indicate that an increase of the amount of Al in contact with the DETA amine prior to reaction with DGEBA has the same effect as a decrease of the extent of cure of the polymer. The role of chelated aluminum on polyepoxy curing is thus evidenced not only based on T_g considerations but also from the ΔC_p perspective.

It has sometimes been reported that the product $\Delta C_p \cdot T_g$ for polymers could be considered as rather constant in a first approximation, around 115 J/g [28,29]. In our case, this product spans over the range 118-220 J/g, with a mean of 164 ± 38 J/g. Deeper literature investigations showed that a more complex inverse dependency could apply between ΔC_p and T_g [27-28] following an equation of the type:

$$\Delta C_p = a + \frac{b}{T_g} \quad (\text{with } T_g \text{ expressed in Kelvin}) \quad \text{Eq. 2}$$

Plotting here $\Delta C_p = f(T_g)$ leads here (**Figure 1b**) to $a \cong 0 \text{ J.g}^{-1}.\text{K}^{-1}$ and $b \cong 97 \text{ J.g}^{-1}$. Although these values are only rough estimates due to experimental points scattering, they give a first approximation of the relation existing between ΔC_p and T_g for the DGEBA/DETA/Al system. Boyer [28] proposed in the 1970s a general rule with $a \cong 17 \cdot 10^{-2} \text{ J.g}^{-1}.\text{K}^{-1}$ and $b \cong 63 \text{ J.g}^{-1}$ (as recalculated from calories to Joules) from the analysis of 30 polymers. The couple of (a,b) values may, however, depend on the nature of the monomers used. For information, Montserrat [27] reported the values $a \cong 8.9 \cdot 10^{-2} \text{ J.g}^{-1}.\text{K}^{-1}$ and $b \cong 107.2 \text{ J.g}^{-1}$ for the DGEBA/phthalic anhydride system.

In the process of polymer curing, it is possible to relate the extent of cure α to the glass transition temperature T_g via the DiBenedetto equation, re-written by Pascault and Williams [30] in the form:

$$\frac{T_g - T_{g0}}{T_{g\infty} - T_{g0}} = \frac{\lambda \alpha}{1 - (1 - \lambda)\alpha} \quad \text{Eq. 3}$$

where λ is a parameter between 0 and 1 characteristic of the polymer considered, and accessible via $\lambda = \Delta C_{p\infty} / \Delta C_{p0}$. The underscript “ ∞ ” refers to a theoretical infinite molecular

weight, as is customary. In the present case, $\Delta C_{p\infty}$ and ΔC_{p0} have been measured as 0.197 and 0.527 J.g⁻¹.K⁻¹ respectively, leading to $\lambda = 0.374$. It may be noted that this experimental value is lower than ~0.600 that might be considered *a priori* for such systems by analogy with other epoxy systems [30], although values down to 0.42 have for example been reported for DGEBA-based polyepoxys cured with di-amines [30]. Taking into account the measured values of $T_{g\infty} = 131$ °C and $T_{g0} = -42$ °C (see Fritah et al. [24]), application of **Eq. 3** with $\lambda = 0.374$ then leads to the $\alpha = f(T_g)$ curve plotted on **Figure 2a**. This curve may be seen as a characteristic of the DGEBA/DETA system studied here.

Another way to access the value of λ is by considering the glass transition temperature at the gel point. Flory's theory [31] allows determining the gel conversion point from the relationship:

$$\alpha_{gel} = \left(\frac{r}{(f_a - 1)(f_e - 1)} \right)^{1/2} \quad \text{Eq. 4}$$

using the same r and f parameters as described in **Eq.1**. Application to the DGEBA/DETA system, this leads to $\alpha_{gel} = 0.50$. From the $\alpha = f(T_g)$ curve plotted on **Figure 2a**, the glass transition temperature at the gel point can then be evaluated to $T_{g\ gel} \cong 5$ °C. Re-writing **Eq. 3** for the gel point gives $\lambda = 0.373$, thus validating the above value.

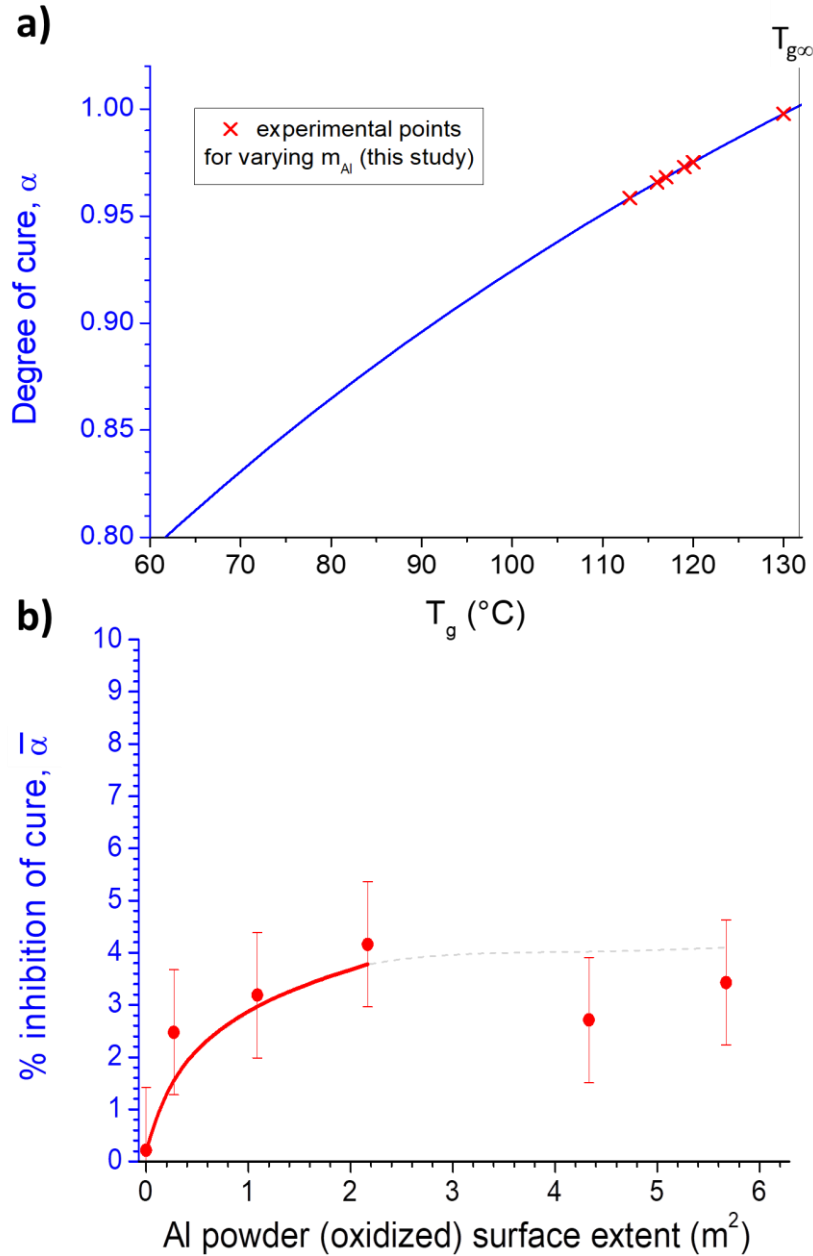


Figure 2. a) Evolution of the extent of cure α versus T_g (with $\lambda = 0.374$, $T_{g0} = -42$ $^{\circ}\text{C}$ as measured and $T_{g\infty} = 131$ $^{\circ}\text{C}$) over the α range 0.8-1 and b) Evolution of the percentage of inhibition of cure $\bar{\alpha}$ for Al in the DETA/DGEBA system, versus the surface extent of Al powder. Stoichiometry corresponds to 1.4 g DETA + 11.8 g DGEBA giving a polymer mass of 13.2 g.

Our previous discussion has, on the other hand, established that contacting DETA with aluminum before polymerization with DGEBA had similar effects as a decrease of the extent of cure. In this context, it appears reasonable to keep the same $\alpha = f(T_g)$ curve as above

(**Figure 2a** and **Figure S4a**) and to determine, from experimental T_g values, the equivalent extent of cure relative to each aluminum mass tested. It is then possible to relate directly α with m_{Al} (**Figure S4b**). Additionally, we propose another way to describe this situation by defining a percentage of inhibition of cure $\bar{\alpha}$ calculated as $\bar{\alpha} = 100 \cdot (1 - \alpha)$. This parameter could indeed prove helpful in the future for comparing more directly the effect of different metals or surface states on epoxy curing. The evolution of $\bar{\alpha}$ with the exposed Al surface is shown on **Figure 2b**. Despite data scattering due to the propagation of uncertainty, in our experimental conditions inhibition up to ~4% was evidenced, with an increasing trend is found for $\bar{\alpha}$ up to about 600 mg Al (for 1.5 ml DETA) which corresponds to 2.22 m² of contact surface. Then, a flattening of the curve is observed for data points corresponding to the highest Al masses tested. This effect will be further commented in the discussion section.

These findings allow deriving a direct correspondence between the amount of aluminum pre-contacted with DETA and the resulting decrease in curing related to the blocking of some amine functions by chelation with Al³⁺ ions.

3.2. Enthalpy of amine-Al reaction from mixing calorimetry

All of the above clearly illustrates how the DETA-Al interaction directly interferes with the extent of cure of the DETA/DGEBA system. In order to inspect further this amine/metal (hydro/oxide) interaction and formation of related interphase, mixing calorimetry was used as an *in situ* probe, in the same approach as we recently reported [24]. A schematic view of the calorimeter setup is depicted on **Figure S5**. From the calorimetric assays run with various Al masses, enthalpies of DETA-Al interaction were determined by integration of the heat flow versus time thermograms (after subtraction of the blank experiment, see experimental section). In the present work, we added in particular some experimental data obtained with Al chips (see a typical thermogram on **Figure 3a**) and compared them with enthalpy values obtained with Al powder. To this aim, in order to take into account the different division states of these samples, ΔH_R was plotted versus the exposed surface area in m² (**Figure 3b**). As for the powders, a clear exothermic event was also measured with the Al chips, and the data points aligned rather well with those of Al powder. Thus, observation of exothermic DETA-Al interaction is not specific to highly divided metallic powder but it also occurs on macroscopic pieces (as we similarly found for T_g changes, see **Table 1**) and can likely be generalized to any Al-based surface.

Another relevant observation is that, over the whole mass range studied, ΔH_R steadily follows a monotonous trend as m_{Al} increases, with a progressively more pronounced exothermic character, as already pointed out in our previous study [24]. This result indicates that exposure of DETA to incremental amounts of Al systematically generates more interphase formation – thus involving more chelate formation as underlined in the introduction section. Such a conclusion can be drawn owing to the *in situ* nature of mixing calorimetry, which may be seen here as a probe for surface (in fact interphase) reactivity.

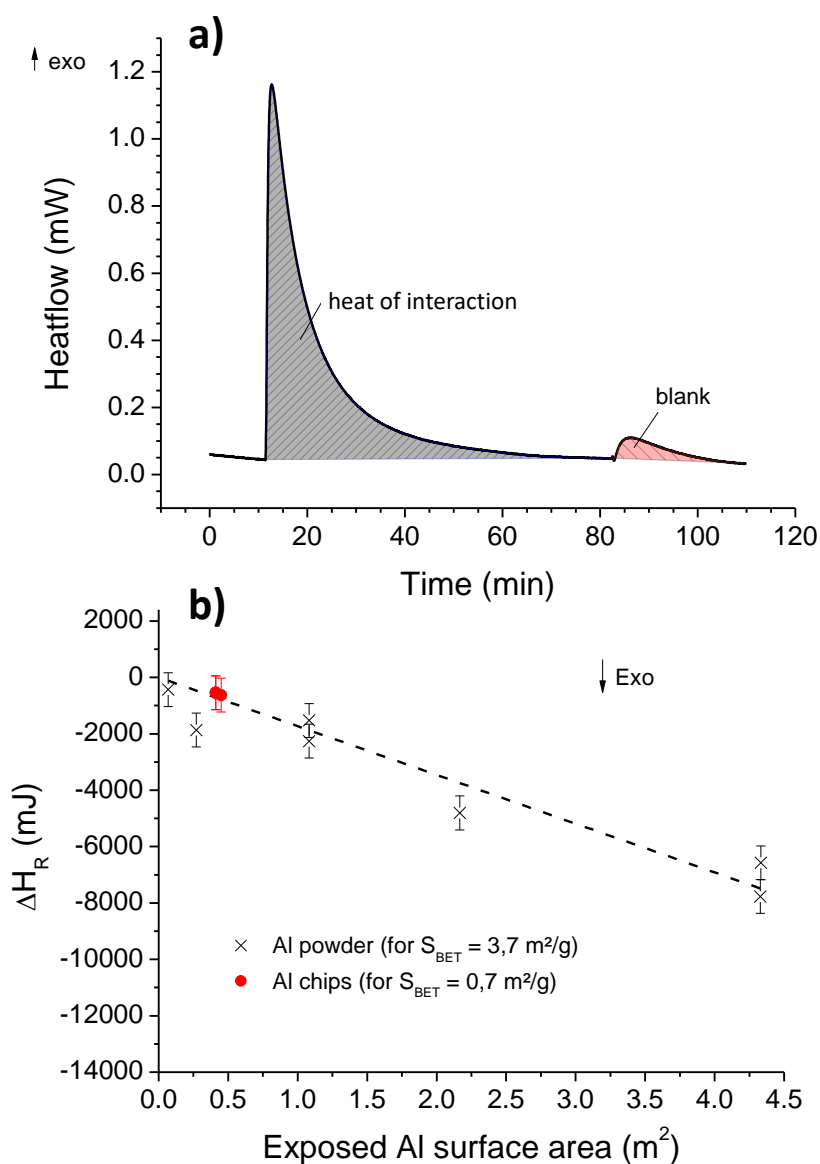


Figure 3. a) Typical thermogram (and calorimeter setup) for mixing calorimetry for Al chips (642 mg Al chips) contacted with 1.5 mL DETA and b) Enthalpy of reaction ΔH_R between DETA and Al powder (x cross points) and chips (● red circles) as a function of exposed surface area.

3.3. Exploration of DETA-aluminum chelate formation from DFT and Raman microscopy

The preceding DSC and mixing calorimetry data have evidenced the direct role of DETA/Al contact on the extent of cure of the DETA/DGEBA system. Chelation of aluminum by DETA at the interphase has been documented in the literature, e.g. on the basis of spectroscopy (XPS, IR) data [6-8,17-21]. A general mechanistic scheme has been proposed in Fritah et al. [24] inspired from previous work [17-19].

Besides, our results show, on the one hand, that the process of DETA/Al interphase formation is exothermic and directly linked to the amount of Al, and on the other hand that it originates an inhibition of cure during subsequent polymerization with DGEBA. The role of DETA/aluminum chelates thus appears fundamental, and should be further scrutinized with the view to progress on the understanding of the role of aluminum on DETA/DGEBA curing. With this in mind, we carried out *ab initio* (DFT) calculations on DETA/aluminum chelates susceptible to form, at least in liquid state, so as to derive a most likely conformational arrangement. We have to note here that, for these preliminary calculations, hypotheses had to be made on the speciation of DETA and aluminum in the formed chelates. At this stage, DETA was considered in its -2 form (loss of two protons) and aluminum in its usual ionic form Al^{3+} . Bearing in mind the molecular structure of the DETA tri-amine, involving two external primary amines (i.e. $-NH_2$ groups in its non-ionized form) and one intermediate secondary amine ($-NH-$), we considered two possible configurations, denoted I and II, as illustrated on **Figure 4**. Configuration I consists in bidentate chelation at one extremity of the DETA molecular ion and involves interaction with both one terminal amine and the intermediate secondary amine (**Figure 4a**). Configuration II, in contrast, implicates the three amine groups as chelating tridentate tweezers (**Figure 4b**), whereas the starting conformation considered Al^{3+} in interaction with the two extreme amine groups. In our previous study, a third configuration had also been suggested *a priori*, (i.e. configuration (a) in Figure 9 from ref. [24]), where Al^{3+} only interacted with the two extreme primary amines in another bidentate chelate without interacting with the central $-NH-$ group of DETA. However, our calculations run with this third configuration rapidly evolved toward the tridentate configuration II, with a significant Al^{3+}/NH spatial interaction. Therefore, this third option was not further considered in the following.

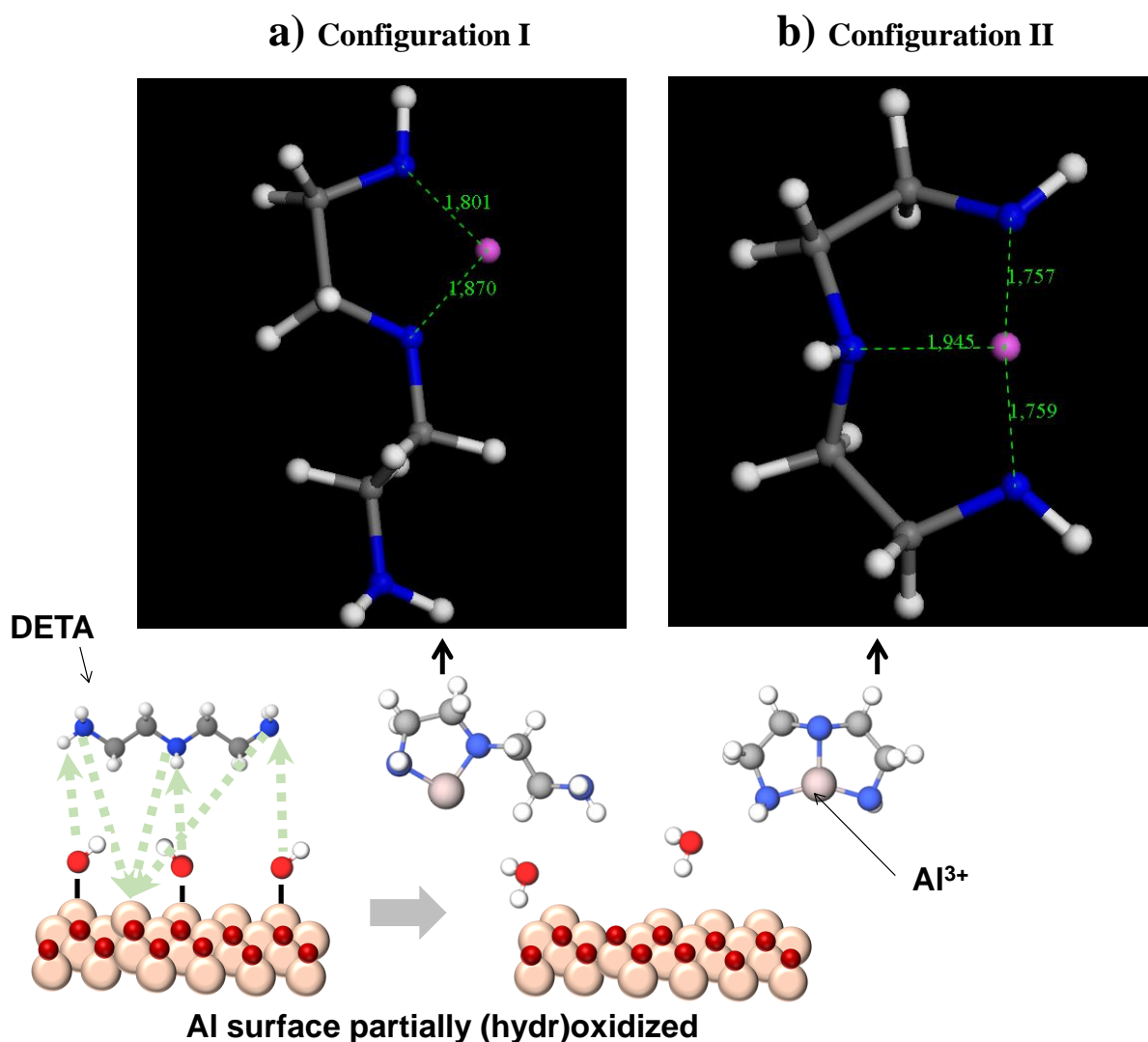


Figure 4. Configurations I and II considered between the DETA tri-amine and an Al^{3+} ion in the DFT calculations (figure background inspired from Fritah et al. [24]).

Computed DFT results in terms of conformational energy E for DETA involved in configurations I and II and in terms of equilibrated Al-N bonds are summarized on **Table 2**. As may be seen, $E(\text{II}) < E(\text{I})$ which is accompanied by a shorter mean Al-N bond length (1.820 versus 1.836 Å). The gain in conformational energy of DETA for configuration II relatively to configuration I is of *ca.* -2,55 eV, thus significant. Therefore, among the two configurations studied configuration II appears as the most stable and likely to form/reside in the liquid DETA.

Table 2. DETA conformational energy E in Al/DETA chelate configurations I and II, and corresponding equilibrium bond lengths between the Al^{3+} ion and the N atoms from DETA, as computed from DFT.

DETA/ Al^{3+} chelate configuration	DETA conformational energy E (eV)	Equilibrated Al-N bond lengths (Å)			
		-NH ₂	-NH-	-NH ₂	Mean value
Configuration I	-565.07065 Ha (-15376.3630 eV)	1.801	1.870	–	1.836
Configuration II	-565.16449 Ha (-15378.9165V)	1.757	1.945	1.759	1.820

Raman spectra were also calculated during the DFT geometry optimization performed on molecular models for these two configurations, along with that of pure DETA (**Figure 5a**). Three main domains may be considered, referred to as domains 1, 2 and 3. The position of bands suggests that domain 1 corresponds essentially to $\nu\text{N-H}$ vibrations, domain 2 mainly to $\nu\text{C-H}$ and domain 3 to a mix of $\delta\text{N-H}$, C-H_{sym} and asym , $\delta\text{C-C}$ and Rocking N-H [32] and/or combination modes. Despite an exaltation of band intensities of domain 3 in configuration I, the main bands occur in the domains 1 and 2. **Figure 5b** and **Figure S6** focus on these calculated spectral regions. As a general trend, a tendency towards higher wavenumbers may be seen for both domains, as indicated by the black arrows, which points to modifications in terms of local constrains, changes in local environment and variations of the electronic distribution (linked to the number of bonds with Al^{3+}). In addition, each domain exhibits different features with rather simple peaks in domain 1 (two bands for pure DETA and config. II and 3 bands for config. I which can be explained by the asymmetric configuration of the config I in which the Al^{3+} interacts only with two amine groups) and a more complex set of partially superimposed components in domain 2. The analysis of the theoretical Raman spectra allowed us to attribute the different bands to the corresponding vibrations in domain 1. In the case of Configuration I, the three increasing Raman frequencies can be attributed respectively to the symmetric elongation of N-H bond for non-interacting amine groups, the vibration of the N-H group for external interacting amine and the antisymmetric elongation of N-H bond for non-interacting amine groups. Regarding the Configuration II, the two increasing Raman frequencies can be attributed to the vibration of N-H central amine group

and to the vibration of N-H external amine groups (which are equivalent).

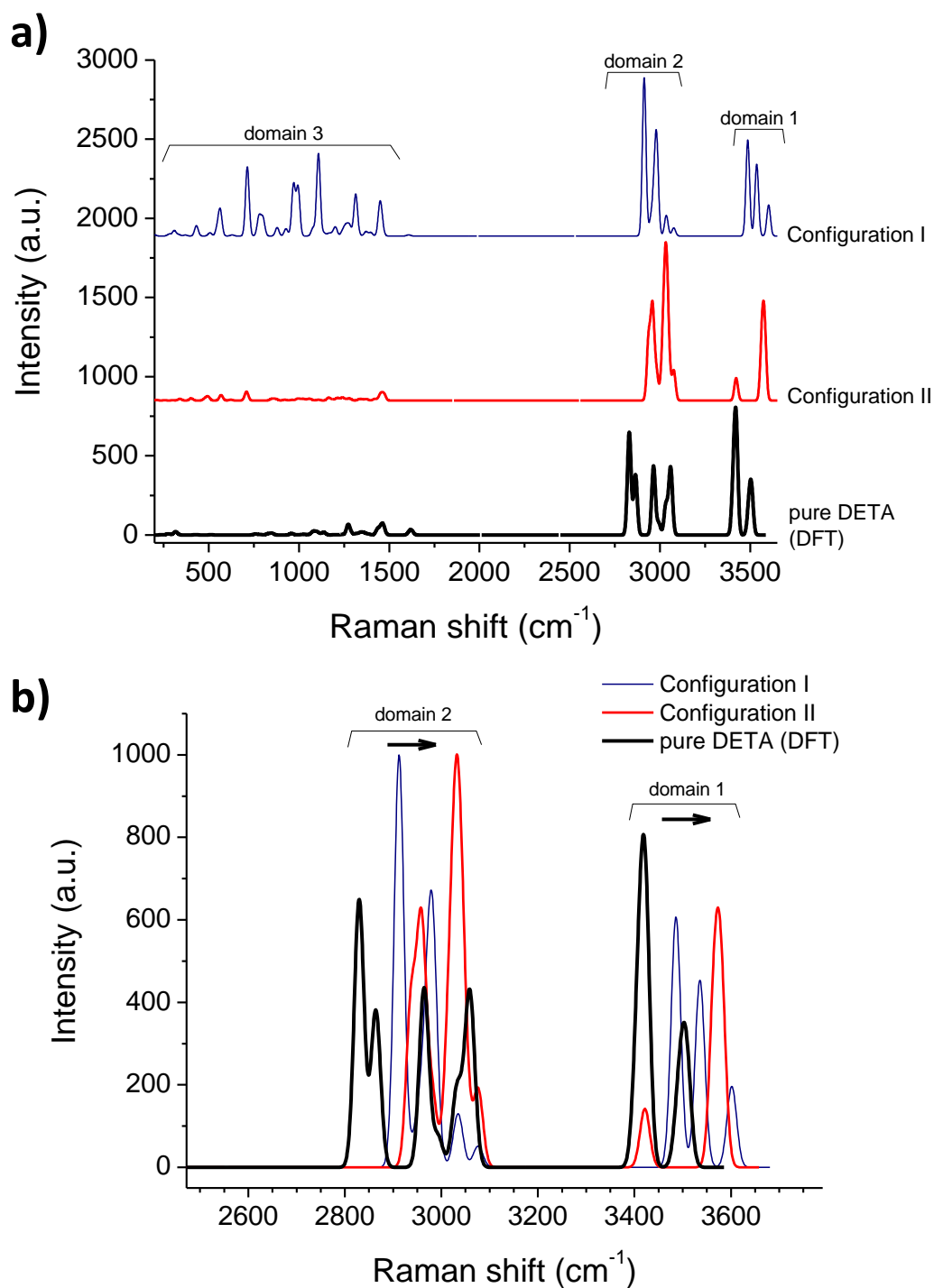


Figure 5. Calculated Raman spectra for configurations I and II as determined from DFT:

a) overall spectra, b) zoom on domains 1 and 2.

In parallel, experimental Raman spectra were also recorded on pure DETA as well as DETA contacted with aluminum (DETA placed between two Al plates for ~72 h). In this latter case, two samplings of DETA were made: i) in the central liquid phase between the two plates and

ii) on a remaining DETA droplet on one Al plate after plates separation. **Figure S7** reports the full spectra recorded with these compounds. In the case of pure DETA, a first comparison between the calculated and experimental spectral features was made (**Figure 6**). Of particular relevance in this comparison is the *shape* of calculated spectral featured rather than their exact position, due to both DFT approximations and non-ideality of experimental outcomes, which allowed us to find optimized superimposition. As for the calculated spectrum of pure DETA, three main domains 1, 2 and 3 can also be distinguished in the experimental spectrum, and a good general accordance may be seen – despite some contributions (marked as * or °) appearing more or less prominent. Such apparent discrepancies may be explained by the fact that DFT calculations were performed here on isolated molecular models and therefore did not take into account the effect of potential DETA-DETA interactions that are likely to affect band intensities.

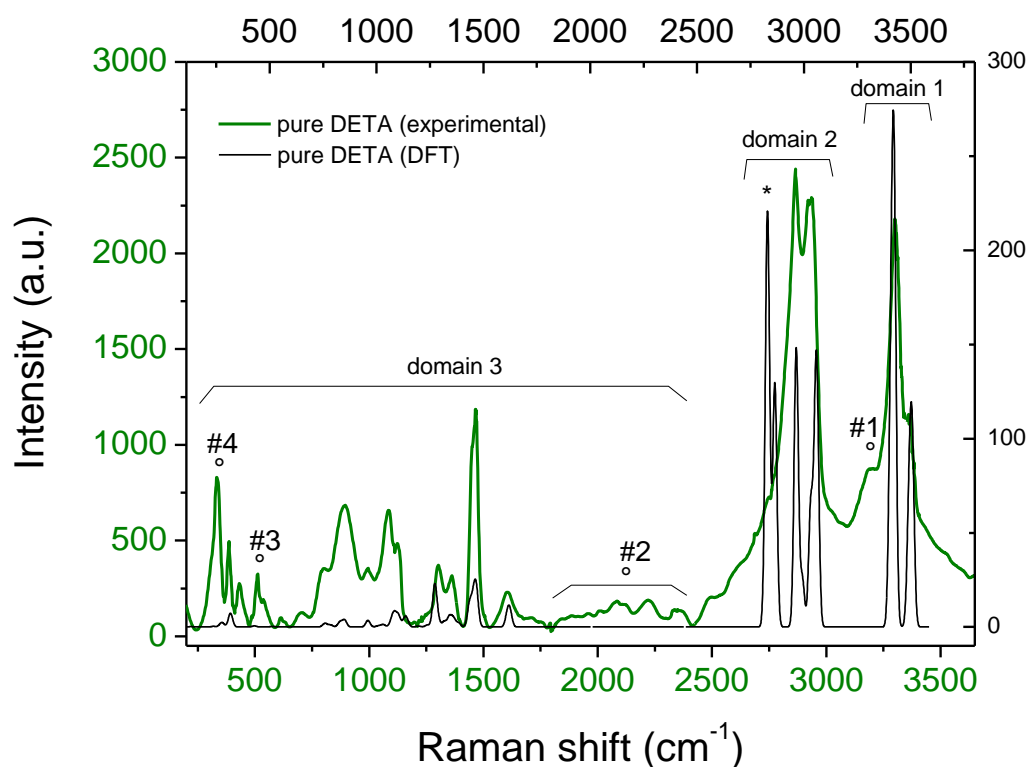


Figure 6. Calculated (DFT) and experimental Raman spectra for pure DETA

In a second stage, a comparison was carried out between the experimental spectrum obtained for pure DETA and the other two DETA samples contacted with Al (**Figure 7**). The two samples involving DETA/Al contact led to similar results, indicating that aluminum was able to diffuse – i.e. under the form of DETA/Al³⁺ chelates) – efficiently within the DETA liquid film between the two Al plates. Compared to pure DETA, several modifications of

experimental Raman features can be underlined. In domain 1 (**Figure 7a**), a shift toward higher wavenumbers was observed associated to a decrease in band width. Rather similar trends were found in domain 2 (**Figure 7b**), and this was accompanied by an inversion of relative intensities as indicated by the pink arrows. This effect could be related to a polarization effect, with modifications of orientations. Again, bands appear thinner than with pure DETA. In domain 3 (**Figure 7c**), some modifications are also noticed with a thinning of the $\delta\text{N-H}$ band at 1600 cm^{-1} , upshift of the $\delta\text{C-H}_{\text{sym}}$ band at 1300 cm^{-1} and downshift of the band at band at 900 cm^{-1} . These observations are likely related to a more constrained chemical environment for DETA contacted with aluminum, which is in accord with the $\text{DETA}/\text{Al}^{3+}$ chelation process.

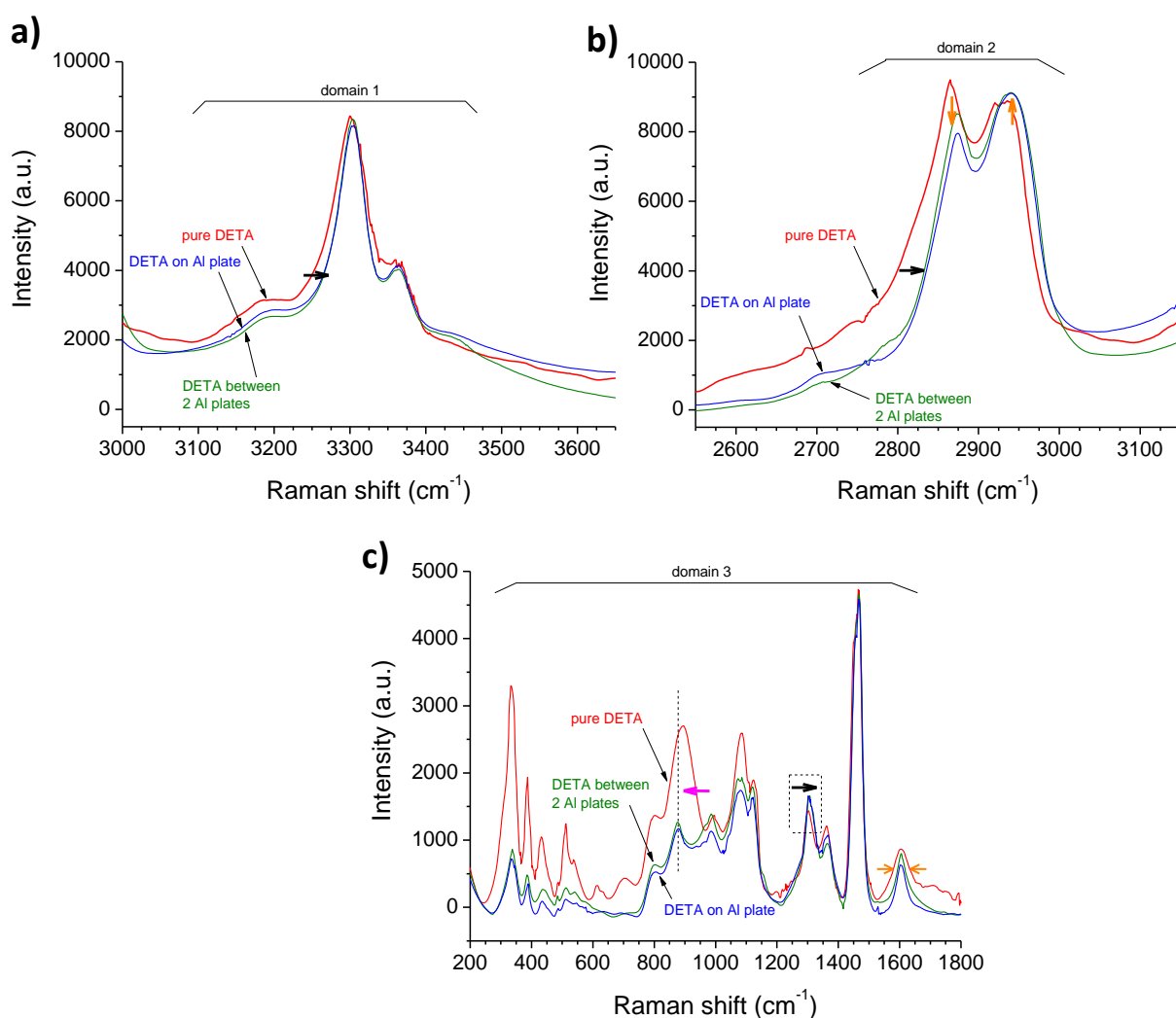


Figure 7. Experimental Raman spectra: comparison of pure DETA with DETA contacted with Al: a) domain 1, b) domain 2 and c) domain 3.

3.4. Discussion

In the present study, we further investigated epoxy-amine/metal interaction with the view to better understand the role of amine/metal interphase on epoxy curing and final thermosetting polymer properties. We focused on the DGEBA/DETA/Al system. According to literature reports, including our own, DETA contacted with aluminum leads to superficial dissolution of the metal (hydr/oxide) via the formation of chelates ultimately desorbed into the liquid phase [6-8,17-21]. In this contribution, we particularly followed by DSC the effect of a variation of the mass of Al (contacted with DETA prior to polymerization with DGEBA) on glass transition features. Not only T_g but also ΔC_p were found to be significantly modified. Addition of Al had a similar effect as a departure from stoichiometry and altered the polyepoxy curing, as evidenced by the $\alpha = f(m_{Al})$ curve that we established. We then derived, as a handy parameter, a percentage of inhibition of cure, $\bar{\alpha}$, reaching up to *ca.* 4% in our working conditions.

In parallel, we used mixing calorimetry – as we first reported recently [24] – as an *in situ* tool to quantify the enthalpy of interaction between DETA and Al with varying masses and division states. In all cases, an exothermic event was evidenced during the interphase formation – in accord with our previous report – whose amplitude monotonously increased with m_{Al} .

The combination of DSC and mixing calorimetry is found particularly relevant. Indeed, while the former gives information on the volume of the polyepoxy matrix, the latter more specifically probes the surface (interphase) effect. Our data indicate that the more Al is contacted with DETA before DGEBA curing (at least in the mass range investigated here), the more exothermic the interphase formation. Therefore, Al systematically gets partially dissolved leading to DETA/aluminum chelates in the liquid phase. The inhibition of cure is also found to increase with m_{Al} , as may be expected; however this parameter tends to stabilize for the highest masses of Al. It is not totally clear at this point whether this apparent stabilizing trend of $\bar{\alpha}$ is an intrinsic characteristic of the system beyond a given threshold of Al (impacting molecular mobility) or if it may be related to external limitations, e.g. in terms of diffusion. Indeed, for T_g determinations versus m_{Al} , a sampling of the DETA (i.e. clear supernatants) contacted with Al during calorimetry experiments was made prior to reaction with DGEBA so as to avoid the presence of solid metal particles during polymerization. Therefore, only part of the liquid DETA “affected” by Al could be used for subsequent DGEBA curing, and this may affect glass transition measurements made with massive

amounts of Al. In contrast, in mixing calorimetry, the totality of the surface of the Al substrate was probed, leading to the response of the total surface in contact with DETA.

In order to shed more light on DETA/aluminum chelation, preliminary DFT calculations were made for two relevant chelate configurations, denoted I and II (in link with our previously reported general scheme, see ref. [24]). A third configuration consisting in Al^{3+} only interacting with the two external primary amine groups without interacting with the central secondary amine was ruled out as it evolved rapidly to configuration II. Conformational energy for DETA involved in the different chelates as well as mean Al-N bond lengths concur to identify configuration II (involving the 3 amine groups of DETA in chelating tridentate tweezers) as the most stable.

Raman spectra were also calculated for the two configurations and compared to experimental spectra for pure DETA and DETA contacted with Al plates. From an experimental point of view, DETA contacted with aluminum was found to exhibit rather similar general patterns to pure DETA, however a detailed analysis pointed out some modifications such as bands thinning and shifting. These observations are likely related to the more constrained conformation of DETA within $\text{DETA}/\text{Al}^{3+}$ chelates compared to free molecular DETA. From a modeling point of view, computed Raman features for configuration II appear closer to pure DETA both in domain 1 (same number of single components) and domain 3 (no major band intensification) while configuration I appeared more marginal. Although it is not straightforward to establish a direct correspondence between experimental and calculated observations at this point, overall the comparison thus tends to support configuration II, which would also agree with the DFT-based stability parameters discussed in **Table 2**. To this date, we believe this is the first proposition of $\text{DETA}/\text{Al}^{3+}$ “stable” chelate conformation, involving interaction of Al^{3+} simultaneously with the three amine groups. Further refinement of calculation methodologies will be interesting to develop in the future for allowing even greater agreement between the experimental and predicted Raman features.

4. Concluding remarks

This work combined experimental analyses by DSC, mixing calorimetry and Raman microscopy with computational chemistry, and allowed clarifying some aspects of epoxy-amine/metal interaction. It also allowed providing first DFT calculations on relevant $\text{DETA}/\text{Al}^{3+}$ chelates in solution. This opens the way to further investigations, still combining experimental and computational approaches, e.g. to scrutinize the effect of $\text{DETA}/\text{Al}^{3+}$ chelates in polymer chain mobility and also to inspect chelate (con)formation on the metal

surface prior to desorption. Extension to the study of other amines and/or less reactive “noble” metals are also planned. Finally, this work could also prove helpful for better apprehending macroscopic effects with epoxy-amine-metal systems, such as the role of filler addition for applicative purposes (e.g. [33]).

Acknowledgements

The authors thank the GDR CNRS 3584 - TherMatHT for fruitful discussions favoring this collaborative work. The authors also want to gratefully thank S. Genty (Université de Toulouse, CIRIMAT and SOCOMORE society) for his preliminary exploration data about DETA-metal interaction using Raman spectroscopy.

References

- [1] Ciechgroup report (2019). Available: <https://ciechgroup.com/en/relacje-inwestorskie/market-environment/organic-segment/epoxy-and-saturated-polyester-resins/>
- [2] Gannon J. A., Seymour R. B., Kirshenbaum G. S.: History and Development of Epoxy Resins. in ‘High Performance Polymers: Their Origin and Development’ (ed.: Kirshenbaum G. S.) Springer, Dordrecht Netherlands, 299-307 (1986).
ISBN 978-94-011-7073-4
- [3] Pascault J.-P., Williams R. J. J.: Epoxy Polymers: New materials and innovations, WILEY-VCH, Weinheim (2010).
ISBN: 978-3-527-32480-4
- [4] Bentadjine S.; Petiaud R.; Roche A. A., Massardier V.: Organo-metallic complex characterization formed when liquid epoxy-diamine mixtures are applied onto metallic substrates, Polymer, 42, 6271-6282 (2001).
[https://doi.org/10.1016/S0032-3861\(01\)00034-9](https://doi.org/10.1016/S0032-3861(01)00034-9)
- [5] Roche A. A.; Bouchet J., Bentadjine S.: Formation of epoxy-diamine/metal interphases, International Journal of Adhesion and Adhesives, 22, 431-441 (2002).

[https://doi.org/10.1016/S0143-7496\(02\)00021-0](https://doi.org/10.1016/S0143-7496(02)00021-0)

[6] Aufray M., Roche A. A.: Is gold always chemically passive: Study and comparison of the epoxy-amine/metals interphases, *Applied Surface Science*, 254, 1936-1941 (2008).

<https://doi.org/10.1016/j.apsusc.2007.07.192>

[7] Aufray M., Roche A. A.: Residual stresses and practical adhesion: effect of organo-metallic complex formation and crystallization, *Journal of Adhesion Science and Technology*, 20, 1889-1903 (2006).

<http://dx.doi.org/10.1163/156856106779116650>

[8] Aufray M., Roche A. A.: Properties of the interphase epoxy-amine / metal : Influences from the nature of the amine and the metal. in: 'Adhesion - Current Research and Application' (ed.: Possart W.) WILEY-VCH, Weinheim Germany, 89-102 (2006).

ISBN: 978-3-527-60710-5

[9] Bockenheimer C., Valeske B., Possart W.: Network structure in epoxy aluminium bonds after mechanical treatment, *International Journal of Adhesion and Adhesives*, 22, 349-356 (2002).

[https://doi.org/10.1016/S0143-7496\(02\)00014-3](https://doi.org/10.1016/S0143-7496(02)00014-3)

[10] Meiser A., Kübel C., Schäfer H., Possart W.: Electron microscopic studies on the diffusion of metal ions in epoxy-metal interphase, *International Journal of Adhesion and Adhesives*, 30, 170-177 (2010).

<https://doi.org/10.1016/j.ijadhadh.2009.12.001>

[11] Possart W., Krüger J. K., Wehlack C., Müller U., Petersen C., Bactavatchalou R., Meiser A.: Formation and structure of epoxy network interphases at the contact to native metal surfaces, *Comptes Rendus Chimie*, 9, 60-79 (2006).

<https://doi.org/10.1016/j.crci.2005.04.009>

[12] Chung J., Munz M., Sturm H.: Amine-cured epoxy surface morphology and interphase with copper: an approach employing electron beam lithography and scanning force microscopy, *Journal of Adhesion Science and Technology*, 19, 1263-1276 (2005).

<https://doi.org/10.1163/156856105774429073>

[13] Chung J., Munz M., Sturm H.: Stiffness variation in the interphase of amine-cured epoxy adjacent to copper microstructures, *Surface and Interface Analysis*, 39, 624-633 (2007).

<https://doi.org/10.1002/sia.2571>

[14] Sperandio C., Arnoult C., Laachachi A., Di Martino J., Ruch D.: Characterization of the interphase in an aluminium/epoxy joint by using controlled pressure scanning electron microscopy coupled with an energy dispersive X-ray spectrometer, *Micron* 41, 105-111 (2010).

<https://doi.org/10.1016/j.micron.2009.10.006>

[15] Aoki M., Shundo A., Okamoto K., Ganbe T., Tanaka K.: Segregation of an amine component in a model epoxy resin at a copper interface, *Polymer Journal* 51, 359-363 (2019).

<https://doi.org/10.1038/s41428-018-0129-4>

[16] Kollek H.: Some aspects of chemistry in adhesion on anodized aluminium, *International Journal of Adhesion and Adhesives*, 5, 75-80 (1985).

[https://doi.org/10.1016/0143-7496\(85\)90019-3](https://doi.org/10.1016/0143-7496(85)90019-3)

[17] Barthés-Labrousse M.-G.: Mechanisms of Formation of the Interphase in Epoxy-Amine/Aluminium Joints, *The Journal of Adhesion*, 88, 699-719 (2012).

<https://doi.org/10.1080/00218464.2012.682933>

[18] Barthés-Labrousse M.-G.: Acid-base characterisation of flat oxide-covered metal surfaces, *Vacuum*, 67, 385-39 (2002).

[https://doi.org/10.1016/S0042-207X\(02\)00209-9](https://doi.org/10.1016/S0042-207X(02)00209-9)

[19] Mercier D., Rouchaud J.-C., Barthés-Labrousse M.-G.: Interaction of amines with native aluminium oxide layers in non-aqueous environment: Application to the understanding of the formation of epoxy-amine/metal interphases, *Applied Surface Science*, 254, 6495-6503 (2008).

<https://doi.org/10.1016/j.apsusc.2008.04.010>

[20] Gadois C., Swiatowska J., Zanna S., Marcus P.: Influence of Titanium Surface Treatment on Adsorption of Primary Amines, *The Journal of Physical Chemistry C*, 117, 1297-1307 (2013).

<https://doi.org/10.1021/jp306786w>

[21] Montois P., Nassiet V., Petit J. A., Baziard Y.: Viscosity effect on epoxy-diamine/metal interphases: Part I: Thermal and thermomechanical behaviour, *International Journal of Adhesion and Adhesives*, 26, 391-399 (2006).

<https://doi.org/10.1016/j.ijadhadh.2005.06.003>

[22] Yamamoto S., Kuwahara R., Aoki M., Shundo A., Tanaka K.: Molecular Events for an Epoxy-Amine System at a Copper Interface, *ACS Applied Polymer Materials* 2, 1474-1481 (2020).

<https://doi.org/10.1021/acsapm.9b01154>

[23] Langeloth M., Sugii T., Böhm M. C., Müller-Plathe F.: Formation of the Interphase of a Cured Epoxy Resin Near a Metal Surface: Reactive Coarse-Grained Molecular Dynamics Simulations, *Soft Materials*, 12, S71-S79 (2014).

<https://doi.org/10.1080/1539445X.2014.963873>

[24] Fritah Z., Drouet C., Thouron C., Aufray M.: Direct evidence of amine-metal reaction in epoxy systems: an in situ calorimetry study of the interphase formation, *Progress in Organic Coatings*, 148, article # 105769 (2020).

<https://doi.org/10.1016/j.porgcoat.2020.105769>

[25] Chandra Singh U., Kollman P. A.: An approach to computing electrostatic charges for molecules, *Journal of Computational Chemistry*, 5, 129-145 (1984).

<https://doi.org/10.1002/jcc.540050204>

[26] Perdew J. P., Burke K., Ernzerhof M.: Generalized Gradient Approximation Made Simple, *Physical Review Letters*, 77, 3865-3868 (1996).

<https://doi.org/10.1103/PhysRevLett.77.3865>

[27] Montserrat S.: Effect of crosslinking density on $\Delta C_p(T_g)$ in an epoxy network, *Polymer*, 36, 435-436 (1995).

[https://doi.org/10.1016/0032-3861\(95\)91337-7](https://doi.org/10.1016/0032-3861(95)91337-7)

[28] Boyer R. F.: $\Delta C_p(T_g)$ and related quantities for high polymers, *Journal of Macromolecular Science, part B*, 7, 487-501 (1973).

<https://doi.org/10.1080/00222347308207880>

[29] Richardson M. J., Savill N. G.: Derivation of accurate glass transition temperatures by differential scanning calorimetry, *Polymer*, 16, 753-757 (1975).

[https://doi.org/10.1016/0032-3861\(75\)90194-9](https://doi.org/10.1016/0032-3861(75)90194-9)

[30] Pascault J. P.; Williams R. J. J.: Glass transition temperature versus conversion relationships for thermosetting polymers, *Journal of polymer science. Part B: Polymer Physics*, 28, 85-95 (1990).

<https://doi.org/10.1002/polb.1990.090280107>

[31] Flory P. J.: Constitution of Three-dimensional Polymers and the Theory of Gelation, *Journal of Physical Chemistry*, 46, 132-140 (1942).

<https://doi.org/10.1021/j150415a016>

[32] Bukowska J.: On the assignment of the NH_2 stretching modes in the vibrational spectrum of formamide, *Spectrochimica Acta Part A: Molecular Spectroscopy*, 35, 985-988 (1979).

[https://doi.org/10.1016/0584-8539\(79\)80023-9](https://doi.org/10.1016/0584-8539(79)80023-9)

[33] Mori K., Hirai N., Ohki Y., Otake Y., Umemoto T., Muto H.: Effects of interaction between filler and resin on the glass transition and dielectric properties of epoxy resin nanocomposites, *IET Nanodielectrics*, 2, 92-96 (2019).

<http://dx.doi.org/10.1049/iet-nde.2018.0041>

SUPPLEMENTARY INFORMATION

Further insight on amine-metal reaction in epoxy systems

M. Aufray, F. Salles, Z. Fritah, O. Marsan, C. Thouron, C. Drouet

Figure S1: Typical XRD pattern for the Al substrate used in this work. Data were acquired for 2 h using an Equinox 100 diffractometer (INEL) with a cobalt anticathode ($\lambda = 1.78897$ Å).

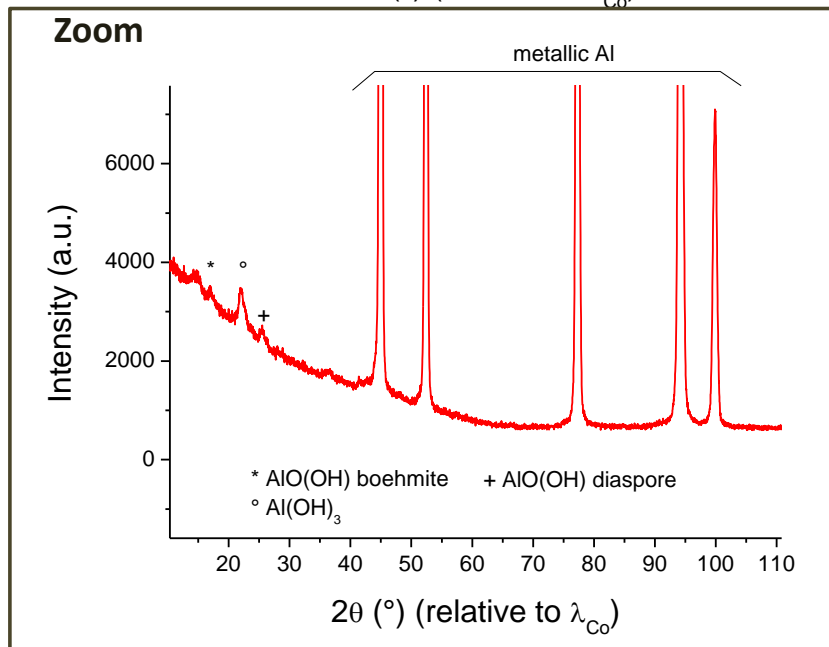
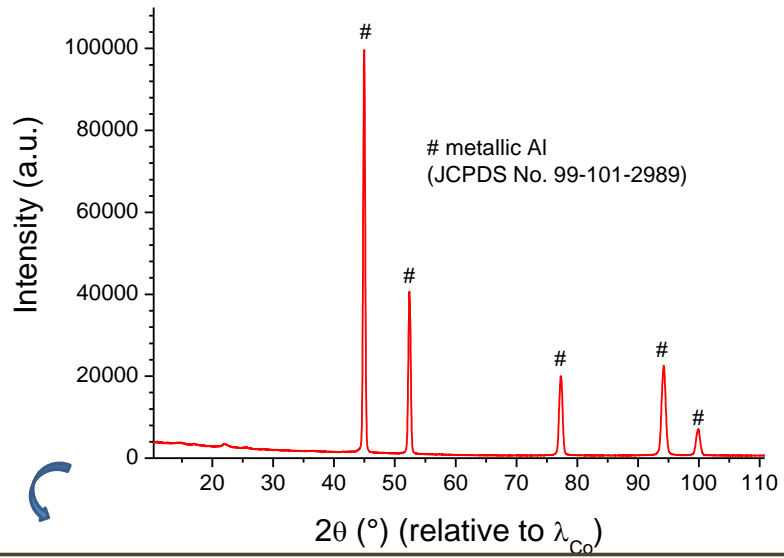
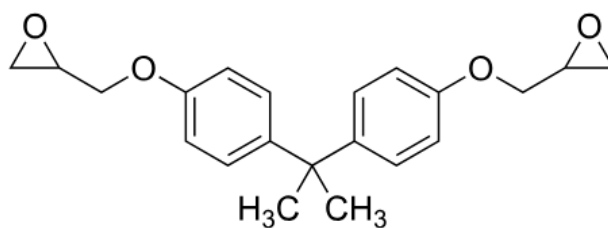


Figure S2: Chemical composition of the DGEBA and DETA monomers used in this study.

- Epoxy monomer: DGEBA



- Amine monomer: DETA

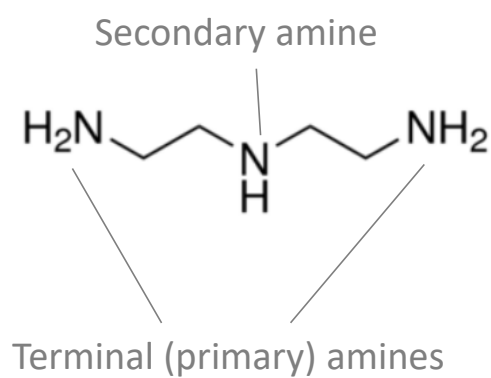


Figure S3: Typical DSC curve for the determination of glass transition features. Data analysis was made with the Proteus® Software allowing us to determine the “onset” and “endset” T_g temperatures by the tangent method as well as the variation in heat capacity, ΔC_p , accompanying the glass transition.

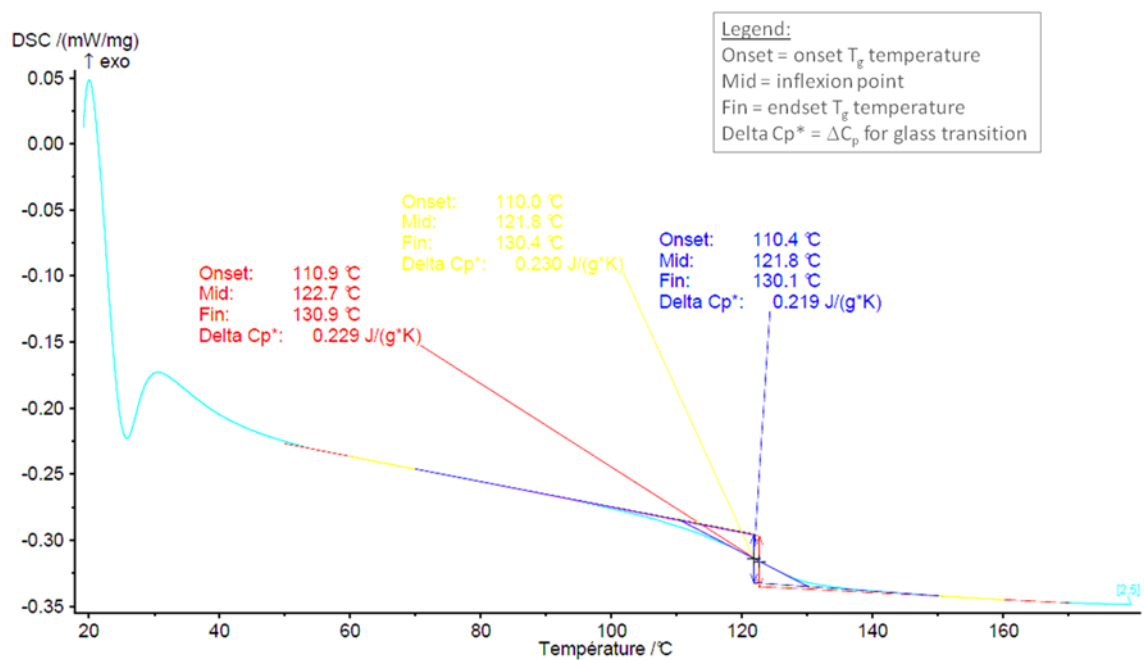


Figure S4: a) Evolution of the extent of cure α versus T_g (with $\lambda = 0.374$, $T_{g0} = -42$ °C as measured and $T_{g\infty} = 131$ °C) over the whole α range 0-1. Calculation of α was performed considering the same $\alpha = f(T_g)$ as for the pure DETA/DGEBA system. b) Evolution of the extent of cure α versus the mass of aluminum m_{Al} contacted with DETA (during mixing calorimetry experiments) prior to polymerization with DGEBA.

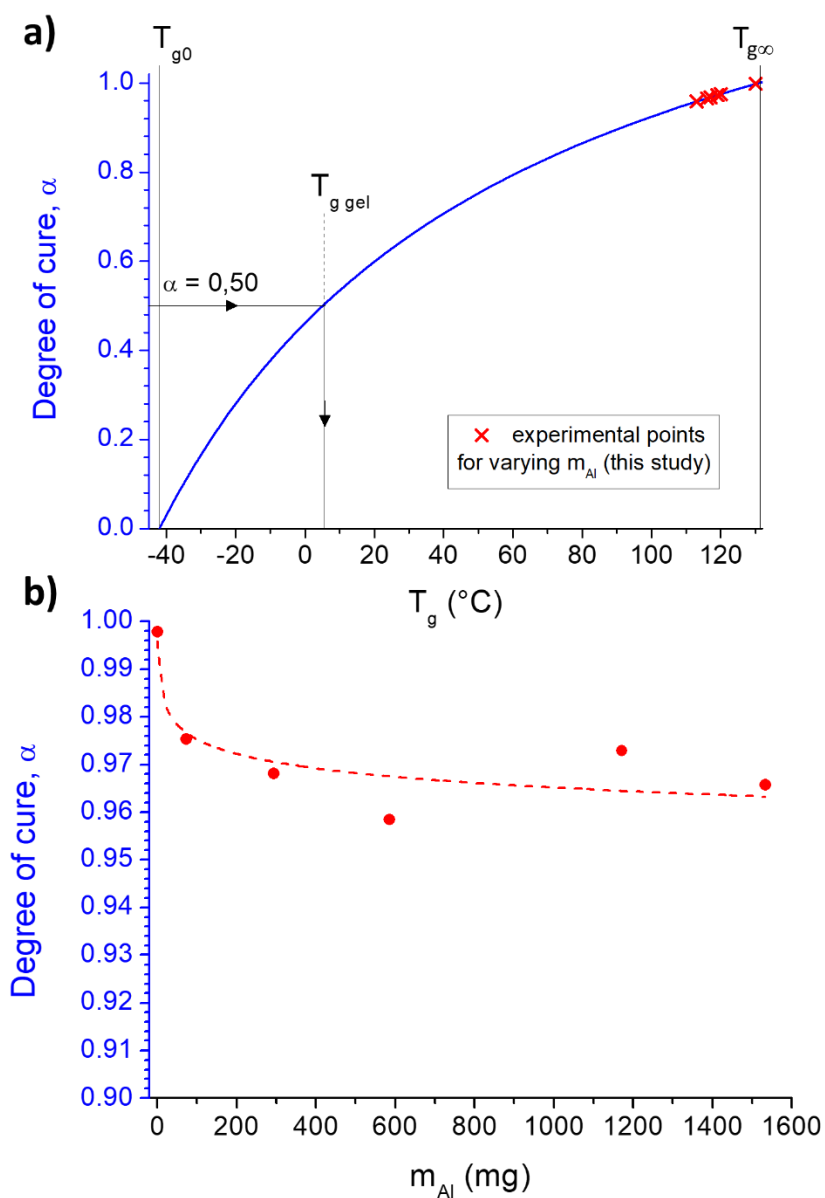


Figure S5: Schematic of a) the DETA/Al interphase studied in this work and b) the calorimeter setup.

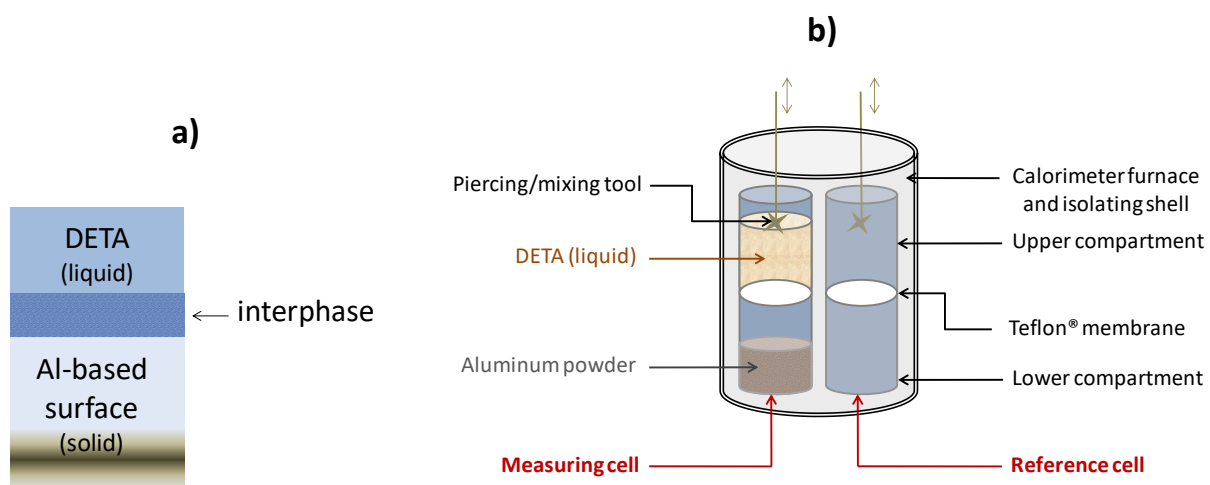


Figure S6: Detailed view on domains 1 (a) and 2 (b) for calculated Raman spectra for pure DETA and DETA/Al³⁺ chelates with configurations I and II.

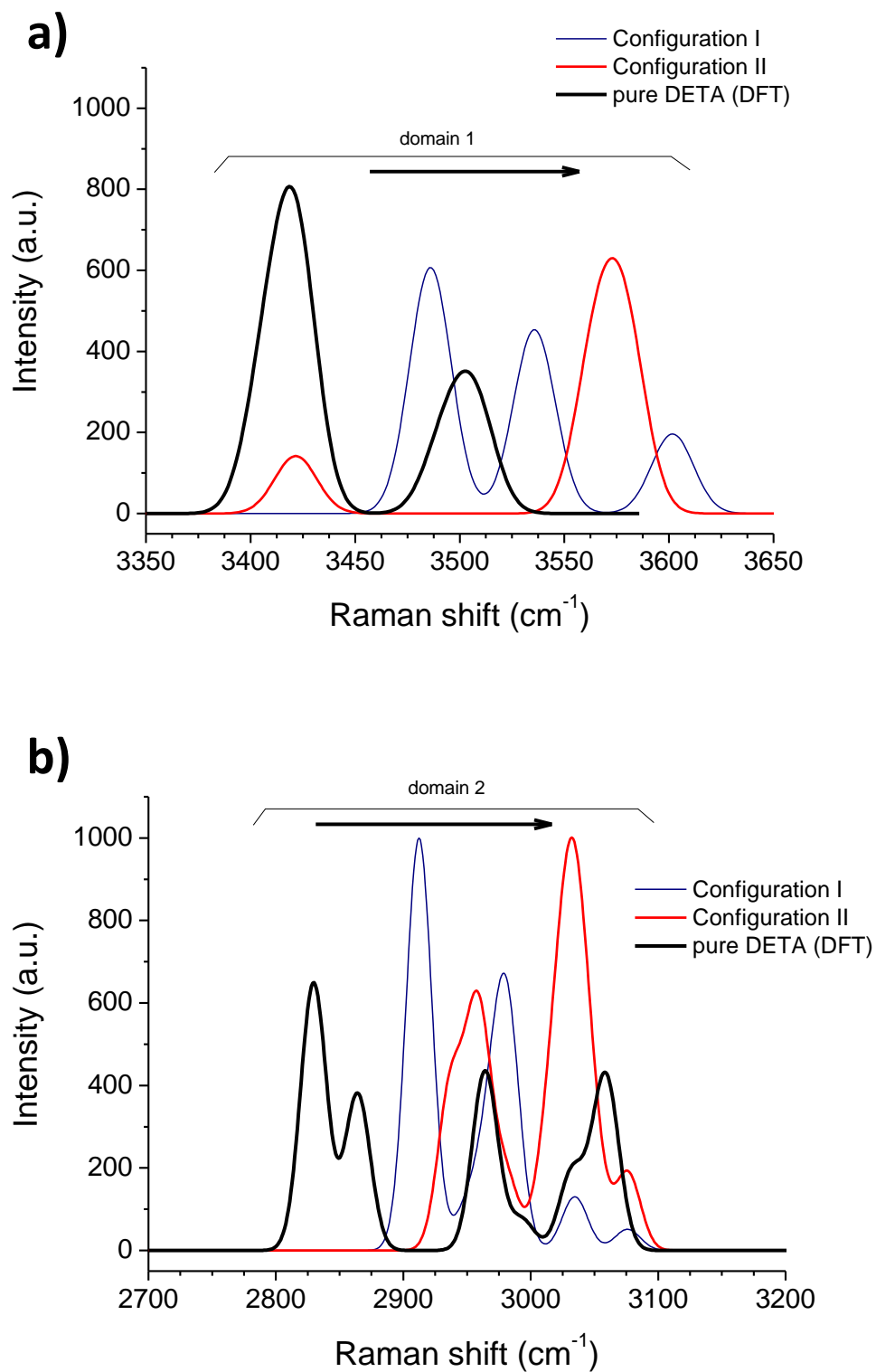


Figure S7: Experimental Raman spectra for pure DETA and DETA contacted with aluminum (DETA placed between two Al plates for ~72 h):

- i) in the central liquid phase between the two plates
- ii) on a remaining DETA droplet on one Al plate after plates separation.

